INTERNATIONAL JOURNAL OF
NUMERICAL ANALYSIS AND MODELING
Volume 14, Number 4-5, Pages 511–531

A THIRD ORDER LINEARIZED BDF SCHEME FOR MAXWELL'S EQUATIONS WITH NONLINEAR CONDUCTIVITY USING FINITE ELEMENT METHOD

CHANGHUI YAO, YANPING LIN, CHENG WANG, AND YANLI KOU

Abstract. In this paper, we study a third order accurate linearized backward differential formula (BDF) type scheme for the nonlinear Maxwell's equations, using the Nédelec finite element approximation in space. A purely explicit treatment of the nonlinear term greatly simplifies the computational effort, since we only need to solve a constant-coefficient linear system at each time step. An optimal L^2 error estimate is presented, via a linearized stability analysis for the numerical error function, under a condition for the time step, $\tau \le C_0^* h^2$ for a fixed constant C_0^*. Numerical results are provided to confirm our theoretical analysis and demonstrate the high order accuracy and stability (convergence) of the linearized BDF finite element method.

Key words. Maxwell's equations with nonlinear conductivity, convergence analysis and optimal error estimate, linearized stability analysis, the third order BDF scheme.

1. Introduction

This paper is concerned with the nonlinear Maxwell's equations

$$\epsilon \mathbf{E}_t + \sigma(\mathbf{x}, |\mathbf{E}|)\mathbf{E} - \nabla \times \mathbf{H} = 0, \ in \ \Omega \times (0, +\infty), \tag{1}$$

$$\mu \mathbf{H}_t + \nabla \times \mathbf{E} = 0, \ in \ \Omega \times (0, +\infty), \tag{2}$$

with initial and boundary conditions

$$\mathbf{E}(\mathbf{x}, 0) = \mathbf{E}_0(x), \ \mathbf{H}(\mathbf{x}, 0) = \mathbf{H}_0(x), \ in \ \Omega, \tag{3}$$

$$\mathbf{n} \times \mathbf{E} = 0 \ \ and \ \ \mathbf{n} \cdot \mathbf{H} = 0, \ on \ \Gamma \times (0, +\infty), \tag{4}$$

where Ω is a bounded, convex, simply-connected domain in R^3 with a regular boundary $\Gamma = \partial\Omega$, $\mathbf{E}(\mathbf{x}, t)$, $\mathbf{H}(\mathbf{x}, t)$ represent the electric and magnetic fields, $\mathbf{n}$ is the outward normal vector on Γ, and the positive constants ϵ and μ stand for the permittivity and the magnetic permeability, respectively. In addition, $\sigma = \sigma(\mathbf{x}, s)$ is a real valued function representing the electric conductivity.

The system $(1)-(4)$ have been investigated in [6, 31, 32]. The authors proved the existence of the weak solution for a nonlinear function $\mathbf{J}(\mathbf{E}) = \sigma(|\mathbf{E}|)\mathbf{E}$, with $\sigma(s)$ monotonically increasing. In [4], the authors presented the existence and uniqueness of the scheme by discretizing the time domain and taking the limit for infinitely small time-step. In section 5 of [4], the authors also proved that the solutions converges to the quasi-state state (no time derivative for equation involving $\mathbf{E}$) when the permittivity $\epsilon \to 0$. Also when ϵ goes zero, numerical example indicated that numerical scheme converges to the quasi static state as part of verification. In [5], the authors proved existence and uniqueness of the discrete fields using the monotone operator theory (see [27]). In [26], the authors studied a time dependent eddy current equation, established the existence and uniqueness of a weak solution in suitable function space, designed a nonlinear time discrete approximation scheme

Received by the editors January 1, 2017 and, in revised form, March 22, 2017.
2000 *Mathematics Subject Classification.* 35R35, 49J40, 60G40.

based on the Rothe's method and proved the convergence of approximation to a weak solution.

Numerical analysis for the nonlinear system have also been extensively carried out, see [2, 3, 4, 5, 9, 10, 11, 12, 13, 14, 18, 22, 23, 25, 26]. In addition, nonlinear schemes have been proposed and analyzed in many literatures. In [4], the authors presented a numerical scheme to solve coupled Maxwell's equations with a nonlinear conductivity, with the backward Euler discretization in time and mixed conforming finite elements in space. And also, a mixed finite element method for the Maxwell's equations with a nonlinear boundary condition was studied in [25]. In [10], the authors proposed a fully-discrete finite element method to solve the time-domain metamaterial Maxwell's equations, which can be reduced to a vector wave integro-differential equation involving just one unknown. Some related works can also be found in [9, 11, 12, 18]. In [5], the authors proposed a numerical scheme based on backward Euler discretization in time and curl-conforming finite element in space to solve Maxwell's equations with nonlinear conductivity in the form of a power law. As a result, its convergence was proved, based on the boundedness of the second derivative in the dual space by the Minty-Browder technique. In [3], the authors developed a fully-discrete $(T, \psi) - \psi_e$ finite element decoupled scheme to solve time-dependent eddy current problem with multiple-connected conductors. Subsequently, an improved convergence rate analysis was provided in [14]. A few more earlier works are also available in [23, 26].

Clearly, linearized schemes are much more efficient than nonlinear schemes for solving nonlinear equations, since only one linear system solver is needed in the former one, while the latter one always requires a nonlinear iteration solver at each time step. For example, a new approach was developed in [16], based on a temporal-spatial error splitting technique by introducing a corresponding time-discrete system. Similarly, a linearized backward differential formula (BDF) type scheme was applied to the time-dependent nonlinear thermistor equation in [7]. The linearized backward Euler scheme for the nonlinear Joule heating equation was studied in [8]. In [29], the authors presented an optimal L^2 error estimate of a linearized Crank-Nicolson Galerkin FEM for a generalized nonlinear Schrödinger equation, without any time step size restriction.

In turn, an important question arises: Is it possible to design higher order (≥ 3) linearized temporal discretization for the nonlinear Maxwell's equations, with a convergence analysis available? In this paper, we give an affirmative answer to this question. We propose a third order accurate, linearized BDF type FEM method for the Maxwell's equations and provide a theoretical error analysis for the proposed scheme. It is well-known that the 3rd order BDF temporal scheme is not A-stable; in fact, its stability domain does not contain any part on the purely imaginary axis, where all the eigenvalues of the linear Maxwell operator are located. This fact makes a theoretical analysis for the 3rd order BDF method applied to the Maxwell equation highly challenging. To overcome this subtle difficulty, we take an inner product with the numerical error equation by $e^{n+1} + (\lambda_0 + 1)(e^{n+1} - e^n)$ (with $\lambda_0 > 0$ and e^k denoted as the numerical error function at time step t^k), and employ a telescope formula established in [20]. Moreover, due to the hyperbolic nature of the Maxwell's equation, a requirement for the time step size, $\tau \leq C_0^* h^2$ (with C_0^* a fixed constant), has to be imposed to pass through the numerical error estimate. Another key technical contribution in the convergence analysis is to obtain an L^∞ bound of the numerical solution, via a linearized stability analysis for the numerical error function; by contrast, such an L^∞ bound was not needed in the previous works [5, 14, 23, 26], due to the implicit treatment of the nonlinear term. In more details, an a-priori L^∞ assumption is made for the numerical error function at the previous time steps, and such an L^∞ bound for the numerical solution leads to a full order $O(\tau^3+h^s)$ error estimate at the next time step. In turn, an application of inverse inequality yields the L^∞ bound of the numerical error function at the next time step, so that an induction could be applied to complete the nonlinear error estimate, under a trivial requirement $\tau \le o(h^{\frac{d}{6}})$. Similar methodology of linearized stability analysis for nonlinear problems could also be found in a few related works [15, 16, 28, 29], etc.

Of course, the time step requirement in the nonlinear error estimate, $\tau \le o(h^{\frac{d}{6}})$, is much less severe than the one imposed for the linear Maxwell part, $\tau \le C_0^* h^2$, associated with the stability analysis for the 3rd order BDF temporal stencil. As a result, the more severe time step constraint, $\tau \le C_0^* h^2$, is needed to pass through the convergence analysis for the whole numerical scheme. Meanwhile, such a severe time step constraint is only a theoretical issue; extensive numerical results have shown that, the stability and convergence are well preserved with a more relaxed constraint, $\tau = O(h)$.

This analysis could easily go through for a polynomial element with degree $s \ge 2$, since the $O(h^s)$ spatial convergence order in L^2 norm enables one to obtain an L^∞ bound of the numerical error function. For a linear element with $s = 1$, such an argument is not directly available. Instead, we perform a super-convergence of the lowest element over a uniform mesh, so that an $O(h^2)$ spatial convergence in L^2 is valid. In turn, an application of inverse inequality yields the desired L^∞ bound for the numerical solution.

The rest of the paper is organized as follows. In Section. 2, we present the linearized BDF finite element method and state the main theoretical result. In Section. 3, we derive an L^2 error estimate of the fully discrete system and get the corresponding estimate of order $O(\tau^3+h^s)$, under a requirement $\tau \le C_0^* h^2$. In particular, the super-convergence analysis for $s = 1$ is also provided in this section. In Section. 4, numerical results are presented to demonstrate the theoretical analysis. Finally, the concluding remarks are provided in Section. 5.

2. Finite element method and the main theoretical result

The inner product in $[L^2(\Omega)]^3$ will be denoted by $(u,v) = \int_\Omega u \cdot v dx$, and the corresponding norm is given by $\|u\| = \sqrt{(u,u)}$. In this article, we use the standard Sobolev spaces and introduce some common notation:

$$\begin{aligned}
&H(curl,\Omega) = \{u \in [L^2(\Omega)]^3; \nabla \times u \in [L^2(\Omega)]^3\},\\
&H_0(curl,\Omega) = \{u \in H(curl,\Omega); \mathbf{n} \times u = 0 \ \ on \ \ \Gamma\},\\
&H(div^0,\Omega) = \{u \in [L^2(\Omega)]^3; div\ u \in L^2(\Omega); div\ u = 0\}.
\end{aligned}$$

Here, we need to employ the assumptions of $\sigma(\mathbf{x},s)$ in [31, 32]. And also, it is assumed that there exist positive constants $\kappa, \sigma_0 > 0$ with $0 < \kappa \le \sigma(\mathbf{x},s) \le \sigma_0$ and $\sigma(\mathbf{x},s) \in C^{1,1}(\Omega,[0,+\infty))$. The problem $(1)-(4)$ has a unique solutions $(\mathbf{E},\mathbf{H})$ such that [6]

$$\begin{aligned}
&\mathbf{E} \in L^2(0,\infty; H_0(curl,\Omega)) \cap H(div^0,\Omega) \cap L^{p+2}(0,\infty;[L^{p+2}(\Omega)]^3),\\
&\mathbf{H} \in L^2(0,\infty; H_0(div^0,\Omega)) \cap H^1(0,\infty;[H^1(\Omega)]^3).
\end{aligned}$$

To introduce the mixed FEM, we partition Ω by a family of regular cubic meshes $\mathcal{T}_h$ with maximum mesh size h. For the spatial approximation, we employ 3D cubic

Raviart-Thomas-Nédelec elements [21, 22]

$$V_h = \{\phi \in H(curl, \Omega), \phi|_K \in Q_{k-1,k,k} \times Q_{k,k-1,k} \times Q_{k,k,k-1}, \forall K \in \mathcal{T}_h\},$$
$$W_h = \{\psi \in [L^2(\Omega)]^3, \psi|_K \in Q_{k,k-1,k-1} \times Q_{k-1,k,k-1} \times Q_{k-1,k-1,k}, \forall K \in \mathcal{T}_h\},$$

or 3D tatrahedron Raviart-Thomas-Nédelec elements

$$V_h = \{\phi \in H(curl, \Omega), \phi|_K \in P_{k-1,k,k} \times P_{k,k-1,k} \times P_{k,k,k-1}, \forall K \in \mathcal{T}_h\},$$
$$W_h = \{\psi \in [L^2(\Omega)]^3, \psi|_K \in P_{k,k-1,k-1} \times P_{k-1,k,k-1} \times P_{k-1,k-1,k}, \forall K \in \mathcal{T}_h\}.$$

In turn, we denote the interpolation operator Π_h and projection operator P_h on V_h and W_h, respectively. The following important properties could be found in [10, 11, 12, 18].

Lemma 2.1. *For the space pairs V_h and W_h, there holds*

$$curl_h V_h \subseteq W_h. \tag{5}$$

If v is a function such that both the interpolants $\Pi_h v$ and $P_h(curl v)$ exist, then we get $curl_h(\Pi_h v) = P_h(curl v)$. For $w \in [L^2(\Omega)]^3$, the following property holds:

$$(w - P_h w, q) = 0, \ \forall q \in W_h.$$

We need the optimal interpolation error estimate [1, 21, 22] for general anisotropically refined meshes. For regular meshes, a similar result is obtained as follows.

Lemma 2.2. *For $1 \leq s \leq k, v \in H^{s+1}(\Omega), w \in H^s(\Omega)$, there exists a constant $C > 0$ independent of h such that*

$$\|v - \Pi_h v\|_{H(curl,\Omega)} \leq Ch^s |v|_{s+1}, \ \|w - P_h w\|_0 \leq Ch^s |w|_s,$$

where $|\cdot|_s$ denotes the seminorm in the space $H^s(\Omega)$.

For $t \in (0, T]$, the weak formulation of $(1)-(2)$ with the boundary condition (4) is defined by

$$(\epsilon \mathbf{E}_t, \xi_u) + (\sigma(\mathbf{x}, |\mathbf{E}|)\mathbf{E}, \xi_u) - (\mathbf{H}, \nabla \times \xi_u) = 0, \ \forall \ \xi_u \in V_h, \tag{6}$$
$$(\mu \mathbf{H}_t, \xi_\phi) + (\nabla \times \mathbf{E}, \xi_\phi) = 0, \ \forall \ \xi_\phi \in W_h. \tag{7}$$

Moreover, let $\{t_n\}_{n=0}^N$ be a partition in time direction with $t_n = n\tau, T = N\tau$ and

$$\mathbf{E}^n = \mathbf{E}(\mathbf{x}, t_n), \qquad \mathbf{H}^n = \mathbf{H}(\mathbf{x}, t_n).$$

For any sequence of functions $\{f^n\}_{n=0}^N$, the third order BDF temporal discrete operator is defined as

$$D_\tau f^n = \frac{1}{\tau}(\frac{11}{6} f^n - 3f^{n-1} + \frac{3}{2} f^{n-2} - \frac{1}{3} f^{n-3}), \ 3 \leq n \leq N. \tag{8}$$

Now, we turn our attention to the computation of the starting approximations. When $n = 0$, we define

$$\mathbf{E}_h^0 = \Pi_h \mathbf{E}_0, \tag{9}$$
$$\mathbf{H}_h^0 = P_h \mathbf{H}_0. \tag{10}$$

In order to compute $(\mathbf{E}_h^1, \mathbf{H}_h^1)$, let $(\widetilde{\mathbf{E}_h^1}, \widetilde{\mathbf{H}_h^1})$ be the solution of the following equations

$$(\epsilon \frac{\widetilde{\mathbf{E}_h^1} - \mathbf{E}_h^0}{\tau}, \xi_u) - (\widetilde{\mathbf{H}_h^1}, \nabla \times \xi_u) + (\sigma(\mathbf{x}, |\mathbf{E}^0|)\mathbf{E}_h^0, \xi_u) = 0, \ \forall \xi_u \in V_h, \tag{11}$$

$$(\mu \frac{\widetilde{\mathbf{H}_h^1} - \mathbf{H}_h^0}{\tau}, \xi_\phi) + (\nabla \times \widetilde{\mathbf{E}_h^1}, \xi_\phi) = 0, \quad \forall \xi_\phi \in W_h. \tag{12}$$

Afterward, $(\mathbf{E}_h^1, \mathbf{H}_h^1)$ (corresponding to $n = 1$) is updated as

$$(13)\qquad (\epsilon\frac{\mathbf{E}_h^1 - \mathbf{E}_h^0}{\tau}, \xi_u) - (\frac{\mathbf{H}_h^1 + \mathbf{H}_h^0}{2}, \nabla\times\xi_u) + \frac{1}{2}(\sigma(\mathbf{x}, |\widetilde{\mathbf{E}_h^1}|)\widetilde{\mathbf{E}_h^1} + \sigma(\mathbf{x}, |\mathbf{E}^0|)\mathbf{E}_h^0, \xi_u) = 0,\ \forall \xi_u \in V_h,$$

$$(14)\qquad (\mu\frac{\mathbf{H}_h^1 - \mathbf{H}_h^0}{\tau}, \xi_\phi) + (\nabla\times(\frac{\mathbf{E}_h^1 + \mathbf{E}_h^0}{2}), \xi_\phi) = 0, \quad \forall \xi_\phi \in W_h.$$

Next, for $n = 2$, $(\mathbf{E}_h^2, \mathbf{H}_h^2)$ is determined by

$$(15)\qquad (\epsilon\frac{\mathbf{E}_h^2 - \mathbf{E}_h^1}{\tau}, \xi_u) - (\frac{\mathbf{H}_h^2 + \mathbf{H}_h^1}{2}, \nabla\times\xi_u) + \frac{1}{2}(3\sigma(\mathbf{x}, |\mathbf{E}_h^1|)\mathbf{E}_h^1 - \sigma(\mathbf{x}, |\mathbf{E}^0|)\mathbf{E}_h^0, \xi_u) = 0,\ \forall \xi_u \in V_h,$$

$$(16)\qquad (\mu\frac{\mathbf{H}_h^2 - \mathbf{H}_h^1}{\tau}, \xi_\phi) + (\nabla\times(\frac{\mathbf{E}_h^2 + \mathbf{E}_h^1}{2}), \xi_\phi) = 0, \quad \forall \xi_\phi \in W_h.$$

With the above numerical solutions at the first two time steps, we introduce the linearized third order BDF finite element method for the nonlinear Maxwell's equations $(1) - (4)$: find $\mathbf{E}_h^n \in V_h, \mathbf{H}_h^n \in W_h, n \geq 3$, such that

$$(17)\qquad (\epsilon D_\tau \mathbf{E}_h^n, \xi_u) - (\mathbf{H}_h^n, \nabla\times\xi_u) + (3\sigma(\mathbf{x}, |\mathbf{E}_h^{n-1}|)\mathbf{E}_h^{n-1} - 3\sigma(\mathbf{x}, |\mathbf{E}_h^{n-2}|)\mathbf{E}_h^{n-2} + \sigma(\mathbf{x}, |\mathbf{E}_h^{n-3}|)\mathbf{E}_h^{n-3}, \xi_u) = 0,\ \forall \xi_u \in V_h,\ n \geq 3,$$

$$(18)\qquad (\mu D_\tau \mathbf{H}_h^n, \xi_\phi) + (\nabla\times\mathbf{E}_h^n, \xi_\phi) = 0,\ \forall \xi_\phi \in W_h.$$

Lemma 2.3. *At each time step, the system* $(9) - (18)$ *is uniquely solvable.*

Proof. Since the linear system generated by (17) and (18) is square, the existence of the solution is implied by its uniqueness. The homogeneous part of scheme $(17) - (18)$ is given by

$$(19)\qquad \frac{11\epsilon}{6}(\mathbf{E}_h^n, \xi_u) - \tau(\mathbf{H}_h^n, \nabla\times\xi_u) = 0,\ \forall\ \xi_u \in V_h,$$

$$(20)\qquad \frac{11\mu}{6}(\mathbf{H}_h^n, \xi_\phi) + \tau(\nabla\times\mathbf{E}_h^n, \xi_\phi) = 0,\ \forall\ \xi_\phi \in W_h.$$

By choosing $\xi_u = \mathbf{E}_h^n, \xi_\phi = \mathbf{H}_h^n$ in (19) and (20), we have

$$(21)\qquad \frac{11\epsilon}{6}\|\mathbf{E}_h^n\|^2 + \frac{11\mu}{6}\|\mathbf{H}_h^n\|^2 = 0,$$

which in turn yields $\mathbf{E}_h^n = 0, \mathbf{H}_h^n = 0$. The existence and the uniqueness of $(9)-(16)$ can be similarly proved. This completes the proof of Lemma 2.3. $\square$

In the rest part of this paper, the following regularity is assumed for the exact solution of the initial boundary value problem $(1) - (4)$:

$$(22)\qquad \|\mathbf{E}_0\|_{H^s(\Omega)} + \|\mathbf{E}_t\|_{L_\infty(0,T;H^s(\Omega))} + \|\mathbf{E}_t\|_{L_2(0,T;H^s(\Omega))} + \|\mathbf{E}_{tt}\|_{L_2(0,T;H^s(\Omega))} + \|\mathbf{E}_{ttt}\|_{L_2(0,T;H^s(\Omega))} + \|\mathbf{E}_{tttt}\|_{L_2(0,T;H^s(\Omega))} \leq C,$$

$$(23)\qquad \|\mathbf{H}_0\|_{H^s(\Omega)} + \|\mathbf{H}_t\|_{L_\infty(0,T;H^s(\Omega))} + \|\mathbf{H}_t\|_{L_2(0,T;H^s(\Omega))} + \|\mathbf{H}_{tt}\|_{L_2(0,T;H^s(\Omega))} + \|\mathbf{H}_{ttt}\|_{L_2(0,T;H^s(\Omega))} + \|\mathbf{H}_{tttt}\|_{L_2(0,T;H^s(\Omega))} \leq C.$$

We present the main theoretical result in the following theorem.

Theorem 2.1. *Let* $(\mathbf{E}, \mathbf{H})$ *be the solution of the problem* $(1)-(4)$*, with the regularity given by* $(22) - (23)$*,* $(\mathbf{E}_h^n, \mathbf{H}_h^n)$ *be the solution of the discrete scheme* $(17) - (18)$ *and starting approximations* $(9) - (16)$*, with the finite element polynomial degree*

$2 \leq s \leq k$. *Under the requirement that* $\tau \leq C_0^* h^2$, *with* C_0^* *a fixed constant, we have*

$$\|\mathbf{E}^n - \mathbf{E}_h^n\|_0 + \|\mathbf{H}^n - \mathbf{H}_h^n\|_0 \leq C(\tau^3 + h^s), \tag{24}$$

where C *is a positive constant, independent of* n, *the maximum mesh size* h *and time step* τ.

3. The convergence analysis

3.1. Higher Raviart-Thomas-N*é*delec elements. In this section, we provide an error estimate for the linearized BDF Maxwell FEM scheme $(17) - (18)$. As a first step, the starting error estimates are needed.

Lemma 3.1. *Suppose that* $(\mathbf{E}, \mathbf{H})$ *is the solution of problem* $(1) - (4)$ *satisfying* $(22) - (23)$, *with the finite element polynomial degree* $2 \leq s \leq k$. *Then the following error estimates of equations* $(9) - (16)$, *for* $m = 0, 1, 2$, *are valid:*

$$\max_{0 \leq m \leq 2} \|\mathbf{E}^m - \mathbf{E}_h^m\|_0 + \max_{0 \leq m \leq 2} \|\mathbf{H}^m - \mathbf{H}_h^m\|_0 \leq C(\tau^3 + h^s), \tag{25}$$

where C *is a positive constant, independent of* n, h *and* τ.

Proof. The constructed solution $(\widetilde{\mathbf{E}^1}, \widetilde{\mathbf{H}^1})$ and its interpolation $(\Pi_h \widetilde{\mathbf{E}^1}, P_h \widetilde{\mathbf{H}^1})$ satisfy the numerical scheme $(11) - (12)$ up to an $O(\tau + h^s)$ truncation error:

$$\begin{aligned} &\epsilon\Big(\frac{\Pi_h \widetilde{\mathbf{E}^1} - \Pi_h \mathbf{E}^0}{\tau}, \xi_u\Big) - (P_h \widetilde{\mathbf{H}^1}, \nabla \times \xi_u) + (\sigma(\mathbf{x}, |\Pi_h \mathbf{E}^0|)\Pi_h \mathbf{E}^0, \xi_u) \\ &\quad = (A, \xi_u), \ \forall\ \xi_u \in V_h, \end{aligned} \tag{26}$$

$$\mu\Big(\frac{P_h \widetilde{\mathbf{H}^1} - P_h \mathbf{H}^0}{\tau}, \xi_\phi\Big) + (\nabla \times \Pi_h \widetilde{\mathbf{E}^1}, \xi_\phi) = (P, \xi_\phi), \ \forall\ \xi_\phi \in W_h, \tag{27}$$

where

$$(A, \xi_u) = (A_1, \xi_u) - (A_2, \nabla \times \xi_u) + (A_3, \xi_u), \tag{28}$$

$$A_1 = \epsilon\Big(\frac{\Pi_h \widetilde{\mathbf{E}^1} - \widetilde{\mathbf{E}^1}}{\tau} + \frac{\widetilde{\mathbf{E}^1} - \mathbf{E}^0}{\tau} - \mathbf{E}_t^{\frac{1}{2}}\Big) + \nabla \times \mathbf{H}^{\frac{1}{2}} - \nabla \times \widetilde{\mathbf{H}^1}, \tag{29}$$

$$A_2 = P_h \widetilde{\mathbf{H}^1} - \widetilde{\mathbf{H}^1}, \tag{30}$$

$$A_3 = \sigma(\mathbf{x}, |\Pi_h \mathbf{E}^0|)\Pi_h \mathbf{E}^0 - \sigma(\mathbf{x}, |\mathbf{E}^0|)\mathbf{E}^0 + \sigma(\mathbf{x}, |\mathbf{E}^0|)\mathbf{E}^0 - \sigma(\mathbf{x}, |\mathbf{E}^{\frac{1}{2}}|)\mathbf{E}^{\frac{1}{2}}, \tag{31}$$

$$\begin{aligned} P = {} & \mu\Big(\frac{P_h \widetilde{\mathbf{H}^1} - \widetilde{\mathbf{H}^1}}{\tau} + \frac{\widetilde{\mathbf{H}^1} - \mathbf{H}^0}{\tau} - \mathbf{H}_t^{\frac{1}{2}}\Big) + \nabla \times \Pi_h \widetilde{\mathbf{E}^1} - \nabla \times \widetilde{\mathbf{E}^1} \\ & + \nabla \times \widetilde{\mathbf{E}^1} - \nabla \times \mathbf{E}^{\frac{1}{2}}. \end{aligned} \tag{32}$$

Based on the interpolation error estimates in Lemmas 2.1- 2.2 and the Taylor expansion, it is easy to see that

$$\|A_1\|_0 \leq C(\tau + h^s), \ (A_2, \nabla \times \xi_u) = 0, \ \|P\|_0 \leq C(\tau + h^s). \tag{33}$$

For the estimate of A_3, with the smooth properties of $\sigma(\mathbf{x}, s)$, the regularity of the exact solution $\mathbf{E}$ and the interpolation error estimates, we have

$$\begin{aligned} & \|\sigma(\mathbf{x}, |\mathbf{E}^0|)\mathbf{E}^0 - \sigma(\mathbf{x}, |\mathbf{E}^{\frac{1}{2}}|)\mathbf{E}^{\frac{1}{2}}\|_0 \\ = {} & \|\sigma(\mathbf{x}, |\mathbf{E}^0|)\mathbf{E}^0 - \sigma(\mathbf{x}, |\mathbf{E}^0|)\mathbf{E}^{\frac{1}{2}} + \sigma(\mathbf{x}, |\mathbf{E}^0|)\mathbf{E}^{\frac{1}{2}} - \sigma(\mathbf{x}, |\mathbf{E}^{\frac{1}{2}}|)\mathbf{E}^{\frac{1}{2}}\|_0 \\ \leq {} & \|\sigma(\mathbf{x}, |\mathbf{E}^0|)(\mathbf{E}^0 - \mathbf{E}^{\frac{1}{2}})\|_0 + \|(\sigma(\mathbf{x}, |\mathbf{E}^0|) - \sigma(\mathbf{x}, |\mathbf{E}^{\frac{1}{2}}|))\mathbf{E}^{\frac{1}{2}}\|_0 \\ \leq {} & \|\sigma(\mathbf{x}, |\mathbf{E}^0|)\|_{L^\infty}\|\mathbf{E}^0 - \mathbf{E}^{\frac{1}{2}}\|_0 + C\|\mathbf{E}^0 - \mathbf{E}^{\frac{1}{2}}\|_0 \|\mathbf{E}^{\frac{1}{2}}\|_{L^\infty} \\ \leq {} & \|\mathbf{E}^0 - \mathbf{E}^{\frac{1}{2}}\|_0 \leq C\tau, \end{aligned} \tag{34}$$

and

$$
\begin{aligned}
(35)\quad & \|\sigma(\mathbf{x},|\Pi_h\mathbf{E}^0|)\Pi_h\mathbf{E}^0-\sigma(\mathbf{x},|\mathbf{E}^0|)\mathbf{E}^0\|_0 \\
= \quad & \|\sigma(\mathbf{x},|\Pi_h\mathbf{E}^0|)\Pi_h\mathbf{E}^0-\sigma(\mathbf{x},|\Pi_h\mathbf{E}^0|)\mathbf{E}^0+\sigma(\mathbf{x},|\Pi_h\mathbf{E}^0|)\mathbf{E}^0-\sigma(\mathbf{x},|\mathbf{E}^0|)\mathbf{E}^0\|_0 \\
\le \quad & \|\sigma(\mathbf{x},|\Pi_h\mathbf{E}^0|)(\Pi_h\mathbf{E}^0-\mathbf{E}^0)\|_0+\|(\sigma(\mathbf{x},|\Pi_h\mathbf{E}^0|)-\sigma(\mathbf{x},|\mathbf{E}^0|))\mathbf{E}^0\|_0 \\
\le \quad & \|\sigma(\mathbf{x},|\Pi_h\mathbf{E}^0|)\|_{L^\infty}\|\Pi_h\mathbf{E}^0-\mathbf{E}^0\|_0+C\|\Pi_h\mathbf{E}^0-\mathbf{E}^0\|_0\|\mathbf{E}^0\|_{L^\infty} \\
\le \quad & C\|\Pi_h\mathbf{E}^0-\mathbf{E}^0\|_0\le Ch^s.
\end{aligned}
$$

Then we arrive at

$$(36)\qquad \|A_3\|_0\le C(\tau+h^s).$$

By denoting $A=A_1+A_3$, we have $\|A\|_0\le C(\tau+h^s)$, $\|P\|_0\le C(\tau+h^s)$.

Define

$$(37)\qquad \widetilde{e^1}=\Pi_h\widetilde{\mathbf{E}^1}-\widetilde{\mathbf{E}^1_h},\ \widetilde{\eta^1}=P_h\widetilde{\mathbf{H}^1}-\widetilde{\mathbf{H}^1_h}.$$

Subtracting (26) – (27) from (11) – (12) yields

$$
\begin{aligned}
(38)\qquad & \epsilon(\frac{\widetilde{e^1}}{\tau},\xi_u)-(\widetilde{\eta^1},\nabla\times\xi_u)+(\sigma(\mathbf{x},|\Pi_h\mathbf{E}^0|)\Pi_h\mathbf{E}^0-\sigma(\mathbf{x},|\mathbf{E}^0|)\mathbf{E}^0_h,\xi_u) \\
& \quad =(A,\xi_u),\ \forall\xi_u\in V_h, \\
(39)\qquad & \mu(\frac{\widetilde{\eta^1}}{\tau},\xi_\phi)+(\nabla\times\widetilde{e^1},\xi_\phi)=(P,\xi_\phi),\ \forall\xi_\phi\in W_h.
\end{aligned}
$$

Taking $\xi_u=\widetilde{e^1}$ in (38) and $\xi_\phi=\widetilde{\eta^1}$ in (39), summing equations (38) and (39) up, we obtain

$$
\begin{aligned}
(40)\qquad \epsilon(\frac{\widetilde{e^1}}{\tau},\widetilde{e^1})+\mu(\frac{\widetilde{\eta^1}}{\tau},\widetilde{\eta^1}) \quad = \quad & (A,\widetilde{e^1})+(P,\widetilde{\eta^1})-(\sigma(\mathbf{x},|\Pi_h\mathbf{E}^0|)\Pi_h\mathbf{E}^0 \\
& -\sigma(\mathbf{x},|\mathbf{E}^0|)\mathbf{E}^0_h,\widetilde{e^1}).
\end{aligned}
$$

Multiplying equation (40) by τ on both sides, employing Young inequality and (35), we have

$$
\begin{aligned}
(41)\qquad & \epsilon\|\widetilde{e^1}\|_0^2+\mu\|\widetilde{\eta^1}\|_0^2\le\tau\|A\|_0\|\widetilde{e^1}\|_0+\tau\|P\|_0\|\widetilde{\eta^1}\|_0+C\tau\|\Pi_h\mathbf{E}^0-\mathbf{E}^0\|_0\|\widetilde{e^1}\|_0 \\
& \le\frac{\tau^2\|A\|_0^2}{4a_1}+a_1\|\widetilde{e^1}\|_0^2+\frac{\tau^2\|P\|_0^2}{4a_2}+a_2\|\widetilde{\eta^1}\|_0^2+\frac{C\tau^2h^{2s}\|\mathbf{E}^0\|_0^2}{4a_3}+a_3\|\widetilde{e^1}\|_0^2.
\end{aligned}
$$

Moreover, by taking $\epsilon>a_1+a_3,\mu>a_2$, we see that

$$(42)\qquad \|\widetilde{e^1}\|_0^2+\|\widetilde{\eta^1}\|_0^2\le C(\tau^4+h^{2s}).$$

For $n=1$, the exact solution $(\mathbf{E}^1,\mathbf{H}^1)$ and its interpolation $(\Pi_h\mathbf{E}^1,P_h\mathbf{H}^1)$ satisfy the numerical scheme (13) – (14) up to an $O(\tau^2+h^s)$ truncation error:

$$
\begin{aligned}
(43)\qquad & \epsilon(\frac{\Pi_h\mathbf{E}^1-\Pi_h\mathbf{E}^0}{\tau},\xi_u)-(\frac{P_h\mathbf{H}^1+P_h\mathbf{H}^0}{2},\nabla\times\xi_u)+\frac{1}{2}(\sigma(\mathbf{x},|\Pi_h\widetilde{\mathbf{E}^1}|)\Pi_h\widetilde{\mathbf{E}^1} \\
& \quad +\sigma(\mathbf{x},|\Pi_h\mathbf{E}^0|)\Pi_h\mathbf{E}^0,\xi_u)=(B,\xi_u), \\
(44)\qquad & \mu(\frac{P_h\mathbf{H}^1-P_h\mathbf{H}^0}{\tau},\xi_\phi)+(\nabla\times\frac{\Pi_h\mathbf{E}^1+\Pi_h\mathbf{E}^0}{2},\xi_\phi)=(M,\xi_\phi),
\end{aligned}
$$

where

$$(B,\xi_u)=(B_1,\xi_u)-(B_2,\nabla\times\xi_u)+(B_3,\xi_u), \tag{45}$$

$$B_1=\epsilon(\frac{\Pi_h\mathbf{E}^1-\mathbf{E}^1}{\tau}+\frac{\mathbf{E}^1-\mathbf{E}^0}{\tau}-\mathbf{E}_t^{\frac{1}{2}})+\nabla\times\mathbf{H}^{\frac{1}{2}}-\nabla\times\frac{\mathbf{H}^1+\mathbf{H}^0}{2}, \tag{46}$$

$$B_2=\frac{P_h\mathbf{H}^1-\mathbf{H}^1}{2}, \tag{47}$$

$$\begin{aligned}B_3=&\frac{1}{2}(\sigma(\mathbf{x},|\Pi_h\widetilde{\mathbf{E}^1}|)\Pi_h\widetilde{\mathbf{E}^1}+\sigma(\mathbf{x},|\Pi_h\mathbf{E}^0|)\Pi_h\mathbf{E}^0-\sigma(\mathbf{x},|\widetilde{\mathbf{E}^1}|)\widetilde{\mathbf{E}^1}\\&-\sigma(\mathbf{x},|\mathbf{E}^0|)\mathbf{E}^0)+\frac{1}{2}(\sigma(\mathbf{x},|\widetilde{\mathbf{E}^1}|)\widetilde{\mathbf{E}^1}+\sigma(\mathbf{x},|\mathbf{E}^0|)\mathbf{E}^0)-\sigma(\mathbf{x},|\mathbf{E}^{\frac{1}{2}}|)\mathbf{E}^{\frac{1}{2}},\end{aligned} \tag{48}$$

$$\begin{aligned}M=&\mu(\frac{P_h\mathbf{H}^1-\mathbf{H}^1}{\tau}+\frac{\mathbf{H}^1-\mathbf{H}^0}{\tau}-\mathbf{H}_t^{\frac{1}{2}})+\nabla\times\frac{\Pi_h\mathbf{E}^1-\mathbf{E}^1}{2}\\&+\nabla\times\frac{\mathbf{E}^1+\mathbf{E}^0}{2}-\nabla\times\mathbf{E}^{\frac{1}{2}}.\end{aligned} \tag{49}$$

Similarly, the following truncation error estimates are available, based on Lemmas 2.1, 2.2., as well as the Taylor expansion:

$$\|B_1\|_0\le C(\tau^2+h^s),\ (B_2,\nabla\times\xi_u)=0,\ \|M\|_0\le C(\tau^2+h^s). \tag{50}$$

The estimate of B_3 depends on the properties of $\sigma(\mathbf{x},s)$, the regularity assumption of the exact solution $\mathbf{E}$, and the interpolation error estimates; the details are skipped for the sake of brevity:

$$\|B_3\|_0\le C(\tau^2+h^s). \tag{51}$$

Therefore, by defining $B=B_1+B_3$, we have $\|B\|_0\le C(\tau^2+h^s)$, $\|M\|_0\le C(\tau^2+h^s)$. Subsequently, we denote

$$e^1=\Pi_h\mathbf{E}^1-\mathbf{E}_h^1,\quad \eta^1=P_h\mathbf{H}^1-\mathbf{H}_h^1. \tag{52}$$

Subtracting (43) – (44) from (13) – (14) results in

$$\begin{aligned}&\epsilon(\frac{e^1}{\tau},\xi_u)-(\frac{\eta^1}{2},\nabla\times\xi_u)+\frac{1}{2}(\sigma(\mathbf{x},|\Pi_h\widetilde{\mathbf{E}^1}|)\Pi_h\widetilde{\mathbf{E}^1}+\sigma(\mathbf{x},|\Pi_h\mathbf{E}^0|)\Pi_h\mathbf{E}^0\\&-\sigma(\mathbf{x},|\widetilde{\mathbf{E}_h^1}|)\widetilde{\mathbf{E}_h^1}-\sigma(\mathbf{x},|\Pi_h\mathbf{E}^0|)\mathbf{E}_h^0,\xi_u)=(B,\xi_u),\ \forall\xi_u\in V_h,\end{aligned} \tag{53}$$

$$\mu(\frac{\eta^1}{\tau},\xi_\phi)+(\nabla\times\frac{e^1}{2},\xi_\phi)=(M,\xi_\phi),\ \forall\xi_\phi\in W_h. \tag{54}$$

Taking $\xi_u=e^1$ in (53) and $\xi_\phi=\eta^1$ in (54), summing equations (53) and (54), we arrive at

$$\begin{aligned}&\epsilon(\frac{e^1}{\tau},e^1)+\mu(\frac{\eta^1}{\tau},\eta^1)=(B,e^1)+(M,\eta^1)-\frac{1}{2}(\sigma(\mathbf{x},|\Pi_h\widetilde{\mathbf{E}^1}|)\Pi_h\widetilde{\mathbf{E}^1}\\&+\sigma(\mathbf{x},|\Pi_h\mathbf{E}^0|)\Pi_h\mathbf{E}^0-\sigma(\mathbf{x},|\widetilde{\mathbf{E}_h^1}|)\widetilde{\mathbf{E}_h^1}-\sigma(\mathbf{x},|\Pi_h\mathbf{E}^0|)\mathbf{E}_h^0,e^1).\end{aligned} \tag{55}$$

The last four terms of (55) could be rewritten as

$$
\begin{aligned}
(56)\qquad & \frac{1}{2}(\sigma(\mathbf{x},|\Pi_h\widetilde{\mathbf{E}^1}|)\Pi_h\widetilde{\mathbf{E}^1}+\sigma(\mathbf{x},|\Pi_h\mathbf{E}^0|)\Pi_h\mathbf{E}^0-\sigma(\mathbf{x},|\widetilde{\mathbf{E}_h^1}|)\widetilde{\mathbf{E}_h^1} \\
& -\sigma(\mathbf{x},|\Pi_h\mathbf{E}^0|)\mathbf{E}_h^0) \\
= \; & \frac{1}{2}(\sigma(\mathbf{x},|\Pi_h\widetilde{\mathbf{E}^1}|)\Pi_h\widetilde{\mathbf{E}^1}-\sigma(\mathbf{x},|\widetilde{\mathbf{E}_h^1}|)\Pi_h\widetilde{\mathbf{E}^1}+\sigma(\mathbf{x},|\widetilde{\mathbf{E}_h^1}|)\Pi_h\widetilde{\mathbf{E}^1} \\
& -\sigma(\mathbf{x},|\widetilde{\mathbf{E}_h^1}|)\widetilde{\mathbf{E}_h^1})+\frac{1}{2}(\sigma(\mathbf{x},|\Pi_h\mathbf{E}^0|)(\Pi_h\mathbf{E}^0-\mathbf{E}^0)+(\sigma(\mathbf{x},|\Pi_h\mathbf{E}^0|) \\
& -\sigma(\mathbf{x},|\mathbf{E}^0|))\mathbf{E}^0) \\
= \; & \frac{1}{2}((\sigma(\mathbf{x},|\Pi_h\widetilde{\mathbf{E}^1}|)-\sigma(\mathbf{x},|\widetilde{\mathbf{E}_h^1}|))\Pi_h\widetilde{\mathbf{E}^1}+\sigma(\mathbf{x},|\widetilde{\mathbf{E}_h^1}|)(\Pi_h\widetilde{\mathbf{E}^1}-\widetilde{\mathbf{E}_h^1})) \\
& +\frac{1}{2}(\sigma(\mathbf{x},|\Pi_h\mathbf{E}^0|)(\Pi_h\mathbf{E}^0-\mathbf{E}^0)+(\sigma(\mathbf{x},|\Pi_h\mathbf{E}^0|)-\sigma(\mathbf{x},|\mathbf{E}^0|))\mathbf{E}^0),
\end{aligned}
$$

so that the following bound could be obtained:

$$
\begin{aligned}
(57)\qquad & \Big\|\frac{1}{2}(\sigma(\mathbf{x},|\Pi_h\widetilde{\mathbf{E}^1}|)\Pi_h\widetilde{\mathbf{E}^1}+\sigma(\mathbf{x},|\Pi_h\mathbf{E}^0|)\Pi_h\mathbf{E}^0-\sigma(\mathbf{x},|\widetilde{\mathbf{E}_h^1}|)\widetilde{\mathbf{E}_h^1} \\
& -\sigma(\mathbf{x},|\Pi_h\mathbf{E}^0|)\mathbf{E}_h^0)\Big\|_0 \\
\leq \; & \|\Pi_h\widetilde{\mathbf{E}^1}-\widetilde{\mathbf{E}_h^1}\|_0\|\Pi_h\widetilde{\mathbf{E}^1}\|_{L^\infty}+\|\sigma(\mathbf{x},|\widetilde{\mathbf{E}_h^1}|)\|_{L^\infty}\|\Pi_h\widetilde{\mathbf{E}^1}-\widetilde{\mathbf{E}_h^1}\|_0 \\
& +\|\sigma(\mathbf{x},|\Pi_h\mathbf{E}^0|)\|_{L^\infty}\|\Pi_h\mathbf{E}^0-\mathbf{E}^0\|_0+C\|\Pi_h\mathbf{E}^0-\mathbf{E}^0\|_0\|\mathbf{E}^0\|_{L^\infty} \\
\leq \; & C\|\Pi_h\widetilde{\mathbf{E}^1}-\widetilde{\mathbf{E}_h^1}\|_0+C\|\Pi_h\mathbf{E}^0-\mathbf{E}^0\|_0 \\
\leq \; & C\|\widetilde{e^1}\|_0+C\|\Pi_h\mathbf{E}^0-\mathbf{E}^0\|_0.
\end{aligned}
$$

Multiplying (55) by τ on both sides and employing Young inequality, we get

$$
\begin{aligned}
(58)\quad \epsilon\|e^1\|_0^2+\mu\|\eta^1\|_0^2 \;\leq\; & \tau\|B\|_0\|e^1\|_0+\tau\|M\|_0\|\eta^1\|_0+\tau\|\widetilde{e^1}\|_0\|e^1\|_0 \\
& +\tau\|\Pi_h\mathbf{E}^0-\mathbf{E}^0\|_0\|e^1\|_0 \\
\leq\; & \frac{\tau^2\|B\|_0^2}{4b_1}+b_1\|e^1\|_0^2+\frac{\tau^2\|M\|_0^2}{4b_2}+b_2\|\eta^1\|_0^2+\frac{C\tau^2\|\widetilde{e^1}\|_0^2}{4b_3} \\
& +b_3\|e^1\|_0^2+\frac{\tau^2h^{2s}\|\mathbf{E}\|_0^2}{4b_4}+b_4\|e^1\|_0^2.
\end{aligned}
$$

In addition, by taking $b_1,b_2,b_3,b_4>0$ such that $b_1+b_3+b_4<\epsilon,\mu>b_2$, we have

$$
\|e^1\|_0^2+\|\eta^1\|_0^2\leq C(\tau^6+h^{2s}). \tag{59}
$$

The estimates for $n=2$ could be carried out in a similar way. The following result could be derived, and the details are left to interested readers:

$$
\|e^2\|_0^2+\|\eta^2\|_0^2\leq C(\tau^6+h^{2s}). \tag{60}
$$

This finishes the proof of Lemma 3.1. □

In addition, the truncation error estimates for $n\geq 3$ are given below.

Proposition 3.1. *For the exact solution* $(\mathbf{E},\mathbf{H})$*, its interpolation* $(\Pi_h\mathbf{E},P_h\mathbf{H})$ *satisfy the numerical scheme* $(17)-(18)$ *up to an* $O(\tau^3+h^s)$ *truncation error, in a* *weak form:*

$$\epsilon(D_\tau \Pi_h \mathbf{E}^n, \xi_u) - (P_h \mathbf{H}^n, \nabla \times \xi_u) + (3\sigma(\mathbf{x}, |\Pi_h \mathbf{E}^{n-1}|)\Pi_h \mathbf{E}^{n-1} -3\sigma(\mathbf{x}, |\Pi_h \mathbf{E}^{n-2}|)\Pi_h \mathbf{E}^{n-2} + \sigma(\mathbf{x}, |\Pi_h \mathbf{E}^{n-3}|)\Pi_h \mathbf{E}^{n-3}, \xi_u) = (g_1^n, \xi_u), \quad \forall \xi_u \in V_h, \tag{61}$$

$$\mu(D_\tau P_h \mathbf{H}^n, \xi_\phi) + (\nabla \times \Pi_h \mathbf{E}^n, \xi_\phi) = (g_2^n, \xi_\phi), \quad \forall \xi_\phi \in W_h, \tag{62}$$

with $\|g_1^n\|_0, \|g_2^n\|_0 \leq C(\tau^3 + h^s)$.

Proof. Obviously, the interpolation $(\Pi_h \mathbf{E}^n, P_h \mathbf{H}^n)$ satisfy the numerical scheme (61) – (62) with the truncated error formula:

$$(g_1^n, \xi_u) = (R_1^n, \xi_u) - (R_2^n, \nabla \times \xi_u) + (R_3^n, \xi_u), \quad \text{with} \tag{63}$$

$$R_1^n = \epsilon(D_\tau \Pi_h \mathbf{E}^n - D_\tau \mathbf{E}^n + D_\tau \mathbf{E}^n - \mathbf{E}_t^n), \tag{64}$$

$$R_2^n = P_h \mathbf{H}^n - \mathbf{H}^n, \tag{65}$$

$$R_3^n = 3\sigma(\mathbf{x}, |\Pi_h \mathbf{E}^{n-1}|)\Pi_h \mathbf{E}^{n-1} - 3\sigma(\mathbf{x}, |\Pi_h \mathbf{E}^{n-2}|)\Pi_h \mathbf{E}^{n-2} \tag{66}$$

$$+\sigma(\mathbf{x}, |\Pi_h \mathbf{E}^{n-3}|)\Pi_h \mathbf{E}^{n-3} - \sigma(\mathbf{x}, |\mathbf{E}^n|)\mathbf{E}^n, \tag{67}$$

$$g_2^n = \mu(D_\tau P_h \mathbf{H}^n - D_\tau \mathbf{H}^n + D_\tau \mathbf{H}^n - \mathbf{H}_t^n) + \nabla \times \Pi_h \mathbf{E}^n - \nabla \times \mathbf{E}^n. \tag{68}$$

The interpolation error estimates in Lemmas 2.1 and 2.2 indicate that

$$\|R_1^n\|_0 \leq C(\tau^3 + h^s), \ (R_2^n, \nabla \times \xi_u) = 0, \ \|g_2^n\|_0 \leq C(\tau^3 + h^s). \tag{69}$$

In addition, the estimate of R_3^n depends on the smooth properties of $\sigma(\mathbf{x}, s)$, the regularity of the exact solution $\mathbf{E}$ and the interpolation error estimates. We begin with a rewritten form: $R_3^n := S_1 + S_2$, with

$$\begin{aligned} S_1 &= 3\sigma(\mathbf{x}, |\Pi_h \mathbf{E}^{n-1}|)\Pi_h \mathbf{E}^{n-1} - 3\sigma(\mathbf{x}, |\Pi_h \mathbf{E}^{n-2}|)\Pi_h \mathbf{E}^{n-2} \\ &\quad +\sigma(\mathbf{x}, |\Pi_h \mathbf{E}^{n-3}|)\Pi_h \mathbf{E}^{n-3} - \sigma(\mathbf{x}, |\Pi_h \mathbf{E}^n|)\Pi_h \mathbf{E}^n, \\ S_2 &= \sigma(\mathbf{x}, |\Pi_h \mathbf{E}^n|)\Pi_h \mathbf{E}^n - \sigma(\mathbf{x}, |\mathbf{E}^n|)\mathbf{E}^n. \end{aligned} \tag{70}$$

An application of Taylor formula in the third order expansion implies that

$$\|S_1\|_0 \leq C\tau^3. \tag{71}$$

For the term S_2, the interpolation error estimates are applied:

$$\begin{aligned} \|S_2\|_0 &= \|\sigma(\mathbf{x}, |\Pi_h \mathbf{E}^n|)\Pi_h \mathbf{E}^n - \sigma(\mathbf{x}, |\mathbf{E}^n|)\mathbf{E}^n\|_0 \\ &\leq \|\sigma(\mathbf{x}, |\Pi_h \mathbf{E}^n|)(\Pi_h \mathbf{E}^n - \mathbf{E}^n)\|_0 + \|(\sigma(\mathbf{x}, |\Pi_h \mathbf{E}^n|) - \sigma(\mathbf{x}, |\mathbf{E}^n|))\mathbf{E}^n\|_0 \\ &\leq \|\sigma(\mathbf{x}, |\Pi_h \mathbf{E}^n|)\|_{L^\infty} \|\Pi_h \mathbf{E}^n - \mathbf{E}^n\|_0 + C\|\Pi_h \mathbf{E}^n - \mathbf{E}^n\|_0 \|\mathbf{E}^n\|_{L^\infty} \\ &\leq C\|\Pi_h \mathbf{E}^n - \mathbf{E}^n\|_0 \leq Ch^s. \end{aligned} \tag{72}$$

A combination of (71) and (72) leads to

$$\|R_3^n\|_0 \leq C(\tau^3 + h^s). \tag{73}$$

Therefore, by defining $g_1^n = R_1^n + R_3^n$, we complete the proof of Proposition 3.1. $\square$

Next, we present the telescope formula in [20] for the third order BDF temporal discretization operator D_τ in the following lemma.

Lemma 3.2. *With the definition of the BDF temporal discrete operator* D_τ *in* (8), *there exists* c_i, $i = 1, \cdots, 10$, $c_1 \neq 0$, *such that*

$$\begin{aligned} &\tau(D_\tau u^n, 2u^n - u^{n-1}) \\ = \ &\|c_1 u^n\|_0^2 - \|c_1 u^{n-1}\|_0^2 + \|c_2 u^n + c_3 u^{n-1}\|_0^2 - \|c_2 u^{n-1} + c_3 u^{n-2}\|_0^2 \\ &+\|c_4 u^n + c_5 u^{n-1} + c_6 u^{n-2}\|_0^2 - \|c_4 u^{n-1} + c_5 u^{n-2} + c_6 u^{n-3}\|_0^2 \\ &+\|c_7 u^n + c_8 u^{n-1} + c_9 u^{n-2} + c_{10} u^{n-3}\|_0^2. \end{aligned} \tag{74}$$

Now we proceed into the proof of Theorem 2.1.

Proof. The following numerical error functions are defined:

$$e^n = \Pi_h \mathbf{E}^n - \mathbf{E}_h^n, \ \eta^n = P_h \mathbf{H}^n - \mathbf{H}_h^n. \tag{75}$$

In turn, subtracting (17) – (18) from the consistency estimate (61) – (62) yields

$$\begin{aligned} (76) \qquad & \epsilon(D_\tau e^n, \xi_u) - (\eta^n, \nabla \times \xi_u) \\ = \quad & -3(\sigma(\mathbf{x}, |\Pi_h \mathbf{E}^{n-1}|)\Pi_h \mathbf{E}^{n-1} - \sigma(\mathbf{x}, |\mathbf{E}_h^{n-1}|)\mathbf{E}_h^{n-1}, \xi_u) \\ & +3(\sigma(\mathbf{x}, |\Pi_h \mathbf{E}^{n-2}|)\Pi_h \mathbf{E}^{n-2} - \sigma(\mathbf{x}, |\mathbf{E}_h^{n-2}|)\mathbf{E}_h^{n-2}, \xi_u) \\ & -(\sigma(\mathbf{x}, |\Pi_h \mathbf{E}^{n-3}|)\Pi_h \mathbf{E}^{n-3} - \sigma(\mathbf{x}, |\mathbf{E}_h^{n-3}|)\mathbf{E}_h^{n-3}, \xi_u) + (g_1^n, \xi_u) \\ := \quad & B_1(\xi_u) + B_2(\xi_u) + B_3(\xi_u) + (g_1^n, \xi_u), \\ (77) \qquad & \mu(D_\tau \eta^n, \xi_\phi) + (\nabla \times e^n, \xi_\phi) = (g_2^n, \xi_\phi). \end{aligned}$$

Taking $\xi_u = 2e^n - e^{n-1} + \lambda_0(e^n - e^{n-1})$ in (76) and $\xi_\phi = 2\eta^n - \eta^{n-1} + \lambda_0(\eta^n - \eta^{n-1})$ in (77), with certain value $\lambda_0 > 0$, we have

$$\begin{aligned} (78) \qquad & \epsilon(D_\tau e^n, 2e^n - e^{n-1}) + \mu(D_\tau \eta^n, 2\eta^n - \eta^{n-1}) \\ & +\epsilon\lambda_0(D_\tau e^n, e^n - e^{n-1}) + \mu\lambda_0(D_\tau \eta^n, \eta^n - \eta^{n-1}) \\ = \quad & B_1(\xi_u) + B_2(\xi_u) + B_3(\xi_u) + (g_1^n, \xi_u) + (g_2^n, \xi_\phi) \\ & +(\lambda_0 + 1)\left((\nabla \times e^n, \eta^{n-1}) - (\eta^n, \nabla \times e^{n-1})\right). \end{aligned}$$

The first two terms in (78) could be analyzed with the help of identity (74). The two additional terms associated with the temporal difference stencil could be estimates as follows:

$$\begin{aligned} (79) \ (D_\tau e^n, e^n - e^{n-1}) \quad = \quad & \frac{1}{\tau}\Big(\frac{11}{6}\|e^n - e^{n-1}\|_0^2 - \frac{7}{6}(e^n - e^{n-1}, e^{n-1} - e^{n-2}) \\ & +\frac{1}{3}(e^n - e^{n-1}, e^{n-2} - e^{n-3})\Big) \\ \geq \quad & \frac{1}{\tau}\Big(\frac{13}{12}\|e^n - e^{n-1}\|_0^2 - \frac{7}{12}\|e^{n-1} - e^{n-2}\|_0^2 \\ & -\frac{1}{6}\|e^{n-2} - e^{n-3}\|_0^2\Big), \\ (80) \ (D_\tau \eta^n, \eta^n - \eta^{n-1}) \quad \geq \quad & \frac{1}{\tau}\Big(\frac{13}{12}\|\eta^n - \eta^{n-1}\|_0^2 - \frac{7}{12}\|\eta^{n-1} - \eta^{n-2}\|_0^2 \\ & -\frac{1}{6}\|\eta^{n-2} - \eta^{n-3}\|_0^2\Big), \end{aligned}$$

in which the Cauchy inequality has been repeatedly applied.

The last two terms in (78) could be rewritten as

$$\begin{aligned} (\nabla \times e^n, \eta^{n-1}) - (\eta^n, \nabla \times e^{n-1}) \quad = \quad & -(\nabla \times e^n, \eta^n - \eta^{n-1}) \\ & +(\eta^n, \nabla \times (e^n - e^{n-1})). \end{aligned} \tag{81}$$

The first part in (81) could be bounded as

$$\begin{aligned} (82) \qquad & -(\lambda_0 + 1)\tau(\nabla \times e^n, \eta^n - \eta^{n-1}) \\ \leq \quad & \frac{1}{3}\mu\lambda_0\|\eta^n - \eta^{n-1}\|_0^2 + C_{\mu,\lambda}^{(0)}\tau^2\|\nabla \times e^n\|_0^2, \end{aligned}$$

with $C_{\mu,\lambda}^{(0)} = \frac{3(\lambda_0+1)^2}{4\mu\lambda_0}$. Furthermore, an application of the inverse inequality

$$\|\nabla \times e\|_0^2 \leq \hat{C}h^{-2}\|e\|_0^2, \tag{83}$$

implies that

$$C_{\mu,\lambda}^{(0)}\tau^2\|\nabla\times e^n\|_0^2 \le C_{\mu,\lambda}^{(0)}\hat{C}\tau^2 h^{-2}\|e^n\|_0^2 \le C_{\mu,\lambda}^{(1)}\tau\|e^n\|_0^2, \tag{84}$$

with $C_{\mu,\lambda}^{(1)} = \hat{C}C_0^* C_{\mu,\lambda}^{(0)}$, under the requirement that $\tau \le C_0^* h^2$. Going back (82), we get

$$-(\lambda_0+1)\tau(\nabla\times e^n, \eta^n - \eta^{n-1}) \le \frac{1}{3}\mu\lambda_0\|\eta^n-\eta^{n-1}\|_0^2 + C_{\mu,\lambda}^{(1)}\tau\|e^n\|_0^2. \tag{85}$$

The second part in (81) could be similarly analyzed:

$$\begin{aligned} &(\lambda_0+1)\tau(\eta^n, \nabla\times(e^n-e^{n-1})) \\ \le\ & \alpha\tau\|\nabla\times(e^n-e^{n-1})\|_0^2 + \frac{1}{4}(\lambda_0+1)^2\alpha^{-1}\tau\|\eta^n\|_0^2 \\ \le\ & \alpha\hat{C}\tau h^{-2}\|e^n-e^{n-1}\|_0^2 + \frac{1}{4}(\lambda_0+1)^2\alpha^{-1}\tau\|\eta^n\|_0^2, \\ \le\ & \alpha\hat{C}C_0^*\|e^n-e^{n-1}\|_0^2 + \frac{1}{4}(\lambda_0+1)^2\alpha^{-1}\tau\|\eta^n\|_0^2, \end{aligned} \tag{86}$$

for any $\alpha > 0$. Meanwhile, we could choose α with $\alpha\hat{C}C_0^* = \frac{1}{3}\epsilon\lambda_0$, so that the above inequality becomes

$$(\lambda_0+1)\tau(\eta^n, \nabla\times(e^n-e^{n-1})) \le \frac{1}{3}\epsilon\lambda_0\|e^n-e^{n-1}\|_0^2 + C_{\epsilon,\lambda}^{(1)}\tau\|\eta^n\|_0^2, \tag{87}$$

with $C_{\epsilon,\lambda}^{(1)} = \frac{1}{4}(\lambda_0+1)^2\alpha^{-1}$. Consequently, a combination of (81), (85) and (87) leads to

$$\begin{aligned} &(\lambda_0+1)\tau\left((\nabla\times e^n, \eta^{n-1}) - (\eta^n, \nabla\times e^{n-1})\right) \\ \le\ & \frac{1}{3}\mu\lambda_0\|\eta^n-\eta^{n-1}\|_0^2 + \frac{1}{3}\epsilon\lambda_0\|e^n-e^{n-1}\|_0^2 + C_{\mu,\lambda}^{(1)}\tau\|e^n\|_0^2 + C_{\epsilon,\lambda}^{(1)}\tau\|\eta^n\|_0^2, \end{aligned} \tag{88}$$

under the condition $\tau \le C_0^* h^2$.

The rest work is focused on the nonlinear error estimate on the right hand side of (78). We note an L^∞ bound for the exact solution and its interpolation

$$\|\mathbf{E}^k\|_{L^\infty} \le C^*, \quad \|\Pi_h\mathbf{E}^k\|_{L^\infty} \le C^*, \tag{89}$$

in which the second inequality comes from the following estimate

$$\|\mathbf{E}^k - \Pi_h\mathbf{E}^k\|_{L^\infty} \le Ch^{s+1}|\ln h|. \tag{90}$$

An a-priori L^∞ assumption up to time step $t^k, k \le n-1$ We also assume a-priori that the numerical error function for $\mathbf{E}$ has an L^∞ bound at time steps t^k:

$$\|e^k\|_{L^\infty} \le 1,\ k \le n-1, \tag{91}$$

so that an L^∞ bound for the numerical solution $\mathbf{E}_h^k$ is available

$$\|\mathbf{E}_h^k\|_{L^\infty} = \|\Pi_h\mathbf{E}^k - e^k\|_{L^\infty} = \|\Pi_h\mathbf{E}^k\|_{L^\infty} + \|e^k\|_{L^\infty} \le C^* + 1 := \widetilde{C_0}. \tag{92}$$

This assumption will be recovered in later analysis.

For the nonlinear error term, we begin with the following decomposition for $k = n-1$:

$$
\begin{aligned}
&\sigma(\mathbf{x}, |\Pi_h \mathbf{E}^{n-1}|)\Pi_h \mathbf{E}^{n-1} - \sigma(\mathbf{x}, |\mathbf{E}_h^{n-1}|)\mathbf{E}_h^{n-1} \\
= \ & \sigma(\mathbf{x}, |\Pi_h \mathbf{E}^{n-1}|)\Pi_h \mathbf{E}^{n-1} - \sigma(\mathbf{x}, |\mathbf{E}_h^{n-1}|)\Pi_h \mathbf{E}^{n-1} \\
&+\sigma(\mathbf{x}, |\mathbf{E}_h^{n-1}|)\Pi_h \mathbf{E}^{n-1} - \sigma(\mathbf{x}, |\mathbf{E}_h^{n-1}|)\mathbf{E}_h^{n-1} \\
= \ & (\sigma(\mathbf{x}, |\Pi_h \mathbf{E}^{n-1}|) - \sigma(\mathbf{x}, |\mathbf{E}_h^{n-1}|))\Pi_h \mathbf{E}^{n-1} \\
&+\sigma(\mathbf{x}, |\mathbf{E}_h^{n-1}|)(\Pi_h \mathbf{E}^{n-1} - \mathbf{E}_h^{n-1}) \\
= \ & (\sigma(\mathbf{x}, |\Pi_h \mathbf{E}^{n-1}|) - \sigma(\mathbf{x}, |\mathbf{E}_h^{n-1}|))\Pi_h \mathbf{E}^{n-1} + \sigma(\mathbf{x}, |\mathbf{E}_h^{n-1}|)e^{n-1}.
\end{aligned} \tag{93}
$$

Moreover, an application of intermediate value theorem shows that

$$\sigma(\mathbf{x}, |\Pi_h \mathbf{E}^{n-1}|) - \sigma(\mathbf{x}, |\mathbf{E}_h^{n-1}|) = \sigma'(\mathbf{x}, \xi^n)e^{n-1}, \tag{94}$$

with ξ^n between $\Pi_h \mathbf{E}^{n-1}$ and $\mathbf{E}_h^{n-1}$. On the other hand, the following estimates are available

$$\|\Pi_h \mathbf{E}^{n-1}\|_{L^\infty} \le C^*, \ \|\mathbf{E}_h^{n-1}\|_{L^\infty} \le \widetilde{C_0}, \tag{95}$$

which coms from the regularity estimate (89) and the a-priori assumption (92), respectively. Then we get

$$\|\xi^n\|_{L^\infty} \le \|\Pi_h \mathbf{E}^{n-1}\|_{L^\infty} + \|\mathbf{E}_h^{n-1}\|_{L^\infty} \le \widetilde{C_1} := C^* + \widetilde{C_0}. \tag{96}$$

As a consequence, we denote

$$\widetilde{C_2} := \max_{\mathbf{x}\in\Omega, -\widetilde{C_1}\le\theta\le\widetilde{C_1}} |\sigma'(\mathbf{x}, \theta)|, \quad \text{so that } \|\sigma'(\mathbf{x}, \xi^n)\|_{L^\infty} \le \widetilde{C_2}. \tag{97}$$

This in turn implies that

$$
\begin{aligned}
&\|(\sigma(\mathbf{x}, |\Pi_h \mathbf{E}^{n-1}|) - \sigma(\mathbf{x}, |\mathbf{E}_h^{n-1}|))\Pi_h \mathbf{E}^{n-1}\|_0 = \|\sigma'(\mathbf{x}, \xi^n)e^{n-1}\Pi_h \mathbf{E}^{n-1}\|_0 \\
\le \ & \|\sigma'(\mathbf{x}, \xi^n)\|_{L^\infty} \cdot \|\Pi_h \mathbf{E}^{n-1}\|_{L^\infty} \cdot \|e^{n-1}\|_0 \le \widetilde{C_2} C^* \|e^{n-1}\|_0,
\end{aligned} \tag{98}
$$

with the Hölder inequality applied at the second step. The analysis for the second term on the right hand side of (93) is more straightforward. By the L^∞ bound (95) for $\|\mathbf{E}_h^{n-1}\|_{L^\infty}$, we denote

$$\widetilde{C_3} := \max_{\mathbf{x}\in\Omega, -\widetilde{C_0}\le\theta\le\widetilde{C_0}} |\sigma(\mathbf{x}, \theta)|, \quad \text{so that } \|\sigma(\mathbf{x}, |\mathbf{E}_h^{n-1}|)\|_{L^\infty} \le \widetilde{C_3}. \tag{99}$$

An application of Hölder inequality shows that

$$\|\sigma(\mathbf{x}, |\mathbf{E}_h^{n-1}|)e^{n-1}\|_0 \le \|\sigma(\mathbf{x}, |\mathbf{E}_h^{n-1}|)\|_{L^\infty} \cdot \|e^{n-1}\|_0 \le \widetilde{C_3}\|e^{n-1}\|_0. \tag{100}$$

Therefore, a combination of (93), (98) and (100) yields

$$\|\sigma(\mathbf{x}, |\Pi_h \mathbf{E}^{n-1}|)\Pi_h \mathbf{E}^{n-1} - \sigma(\mathbf{x}, |\mathbf{E}_h^{n-1}|)\mathbf{E}_h^{n-1}\|_0 \le \widetilde{C_4}\|e^{n-1}\|_0, \tag{101}$$

where $\widetilde{C_4} = \widetilde{C_2} C^* + \widetilde{C_3}$. As a direct consequence, we obtain the nonlinear error estimate

$$
\begin{aligned}
\tau B_1(\xi_u) &\le 3\widetilde{C_4}\tau\|e^{n-1}\|_0 \cdot \|\xi_u\|_0 \\
&\le C\widetilde{C_4}\tau(\|e^{n-1}\|_0^2 + \|e^n\|_0^2 + \|e^{n-1}\|_0^2),
\end{aligned} \tag{102}
$$

with the Cauchy inequality repeatedly applied.

The following estimates could be similarly derived:

$$
\begin{aligned}
\tau B_2(\xi_u) &\le 3\widetilde{C_4}\tau\|e^{n-2}\|_0 \cdot \|\xi_u\|_0 \\
&\le C\widetilde{C_4}\tau(\|e^{n-2}\|_0^2 + \|e^n\|_0^2 + \|e^{n-1}\|_0^2),
\end{aligned} \tag{103}
$$

$$\tau B_3(\xi_u) \leq \widetilde{C_4}\tau\|e^{n-3}\|_0 \cdot \|\xi_u\|_0 \leq C\widetilde{C_4}\tau(\|e^{n-3}\|_0^2 + \|e^n\|_0^2 + \|e^{n-1}\|_0^2). \tag{104}$$

The truncation error terms could be bounded by an application of Cauchy inequality:

$$\tau(g_1^n, \xi_u) \leq \tau\|g_1^n\|_0 \cdot \|\xi_u\|_0 \leq \frac{1}{2}\|g_1^n\|_0^2 + d_5\tau(\|e^n\|_0^2 + \|e^{n-1}\|_0^2), \tag{105}$$

$$\tau(g_2^n, \xi_\phi) \leq \tau\|g_2^n\|_0 \cdot \|\xi_\phi\|_0 \leq \frac{1}{2}\|g_2^n\|_0^2 + d_5\tau(\|\eta^n\|_0^2 + \|\eta^{n-1}\|_0^2). \tag{106}$$

A substitution of the above estimates into (78) gives

$$\begin{aligned} &\epsilon\tau(D_\tau e^n, 2e^n - e^{n-1}) + \mu\tau(D_\tau \eta^n, 2\eta^n - \eta^{n-1}) \\ &+\epsilon\lambda_0\Big(\frac{3}{4}\|e^n - e^{n-1}\|_0^2 - \frac{7}{12}\|e^{n-1} - e^{n-2}\|_0^2 - \frac{1}{6}\|e^{n-2} - e^{n-3}\|_0^2\Big) \\ &+\mu\lambda_0\Big(\frac{3}{4}\|\eta^n - \eta^{n-1}\|_0^2 - \frac{7}{12}\|\eta^{n-1} - \eta^{n-2}\|_0^2 - \frac{1}{6}\|\eta^{n-2} - \eta^{n-3}\|_0^2\Big) \\ \leq\ & (C\widetilde{C_4} + d_5)\tau(\|e^n\|_0^2 + \|e^{n-1}\|_0^2 + \|e^{n-2}\|_0^2 + \|e^{n-3}\|_0^2) \\ &+C_{\mu,\lambda}^{(1)}\tau\|e^n\|_0^2 + (C_{\epsilon,\lambda}^{(1)} + d_5)\tau\|\eta^n\|_0^2 + d_5\tau\|\eta^{n-1}\|_0^2 + \frac{1}{2}\tau(\|g_1^n\|_0^2 + \|g_2^n\|_0^2). \end{aligned} \tag{107}$$

By using the telescope formula (74) for D_τ, summing in (107), and applying the discrete Gronwall inequality, we have

$$\|e^n\|_0^2 + \|\eta^n\|_0^2 \leq \widetilde{C_5}(\tau^6 + h^{2s}), \tag{108}$$

with $\widetilde{C_5}$ dependent on C^*, independent on τ and h.

Recovery of the a-priori bound (91)**.** With the help of the L^2 error estimate (108) and an application of inverse inequality, the following inequality is available, for $d \leq 3$:

$$\|e^n\|_{L^\infty} \leq \frac{C\|e^n\|_0}{h^{\frac{d}{2}}} \leq \frac{\widetilde{C_6}(\tau^3 + h^s)}{h^{\frac{d}{2}}} \leq C, \tag{109}$$

under a trivial requirement $\tau = o(h^{\frac{d}{6}})$. This requirement is much less severe than the one imposed for the linear Maxwell part, $\tau \leq C_0^* h^2$, associated with the stability analysis for the 3rd order BDF temporal stencil. Then we have finished the proof of Theorem 2.1. □

Remark 3.1. *As can be seen in the theoretical derivation, the time step constraint, $\tau \leq C_0^* h^2$, is needed to justify the stability estimate for the 3rd order BDF temporal stencil. This theoretical difficulty comes from the subtle fact that, the 3rd order BDF scheme is not A-stable in the classical standard; in particular, the stability domain of the 3rd order BDF scheme does not contain any part on the purely imaginary axis in the complex plane. On the other hand, it is well-known that all the eigenvalues associated with the linear part of Maxwell operator are purely imaginary. Therefore, a direct stability analysis for the 3rd order BDF scheme is not available for a hyperbolic equation; in comparison, such an analysis could be carefully derived for the parabolic equations, as reported in* [20].

Instead of a third order accurate scheme, if one uses the second order BDF temporal stencil:

$$
\begin{aligned}
(110)\qquad & (\epsilon\frac{\frac{3}{2}\mathbf{E}_h^n-2\mathbf{E}_h^{n-1}+\frac{1}{2}\mathbf{E}_h^{n-2}}{\tau},\xi_u)-(\mathbf{H}_h^n,\nabla\times\xi_u)+(2\sigma(\mathbf{x},|\mathbf{E}_h^{n-1}|)\mathbf{E}_h^{n-1}\\
& \quad -\sigma(\mathbf{x},|\mathbf{E}_h^{n-2}|)\mathbf{E}_h^{n-2},\xi_u)=0,\ \forall\xi_u\in V_h,\ n\geq 2,\\
(111)\qquad & (\mu\frac{\frac{3}{2}\mathbf{H}_h^n-2\mathbf{H}_h^{n-1}+\frac{1}{2}\mathbf{H}_h^{n-2}}{\tau},\xi_\phi)+(\nabla\times\mathbf{E}_h^n,\xi_\phi)=0,\ \forall\xi_\phi\in W_h,
\end{aligned}
$$

the stability and convergence analyses could be carried out with a much milder time step requirement, $\tau = O(h)$. This improvement is based on the fact that, the 2nd order BDF scheme is A-stable, and its stability domain contains the whole part of the purely imaginary axis in the complex plane.

In addition to the BDF approximation (110)-(111), there have been some other second order accurate temporal schemes, such as Leap-frog (Theorem 3.11 [17]*) and Crank-Nicolson (see the related reference* [30]*), so that the stability estimate is available for a $\tau = O(h)$ requirement. However, a theoretical justification of the stability and convergence analyses for any third order accurate temporal scheme applied to nonlinear Maxwell's equations is still an open problem, and this article provided the first such result, under a severe time step constraint, $\tau \leq C_0^* h^2$.*

On the other hand, such a severe time step constraint is only a theoretical issue; extensive numerical results have shown that, the stability and convergence are well preserved with a more relaxed constraint, $\tau = O(h)$.

There may be other alternative third order accurate temporal schemes for the nonlinear Maxwell's equations, so that the stability and convergence analyses could be theoretically justified under the milder time step requirement, $\tau = O(h)$. This investigation will be undertaken in the authors' future works.

3.2. The lowest Raviart-Thomas-Nédelec element. From the above subsection we observe that the convergence order estimate for g_1^n and g_2^n in (69)-(73) has played a crucial role to recover the a-priori bound (91). In more details, its spatial accuracy has to be stronger than $O(h^{\frac{d}{2}})$, as demonstrated in (109). In order to improve the convergence order for the lowest Raviart-Thomas-Nédelec element, we have to employ the super-convergence analysis for a uniform mesh; see [19] for the related theoretical tools. Now we consider the lowest Raviart-Thomas-Nédelec element space in three dimension

$$
\begin{aligned}
V_h &= \{\phi\in H(curl,\Omega),\phi|_K\in Q_{0,1,1}\times Q_{1,0,1}\times Q_{1,1,0},\forall K\in\mathcal{T}_h\},\\
W_h &= \{\psi\in [L^2(\Omega)]^3,\psi|_K\in Q_{1,0,0}\times Q_{0,1,0}\times Q_{0,0,1},\forall K\in\mathcal{T}_h\}.
\end{aligned}
$$

The following results are needed in the later analysis; the detailed proofs could be found in [18].

Lemma 3.3. *For any $\psi_h\in V_h,\phi_h\in W_h$, denote Π_h and P_h as the interpolation operator on V_h and W_h, respectively, we have*

$$(112)\qquad (\mathbf{E}-\Pi_h\mathbf{E},\psi_h)=O(h^2)\|\mathbf{E}\|_2\cdot\|\psi_h\|_0,$$

$$(113)\qquad (\nabla\times(\mathbf{E}-\Pi_h\mathbf{E}),\phi_h)=O(h^2)\|\mathbf{E}\|_2\cdot\|\phi_h\|_0.$$

There exists a post-processing operator $\Pi_{2h}^1 w \in Q_{1,1,1}(\overline{K}), P_{2h}^1 v \in Q_{1,1,1}(\overline{K})$ [18, 19], *such that*

$$(i)\ \|\Pi_{2h}^1 w - w\|_0 \le Ch^2\|w\|_0,\ \|P_{2h}^1 v - v\|_0 \le Ch^2\|v\|_2, \quad \forall\ w \in [H^2(\Omega)]^2, v \in H^2(\Omega), \tag{114}$$

$$(ii)\ \|\Pi_{2h}^1 w\|_0 \le C\|w\|_0,\ \|P_{2h}^1 v\|_0 \le C\|v\|_0,\ \forall\ w \in V_h, v \in W_h, \tag{115}$$

$$(iii)\ \Pi_{2h}^1 w = \Pi_{2h}^1 \Pi_h w,\ P_{2h}^1 V = P_{2h}^1 P_h v,\ \forall\ w \in V_h, v \in W_h, \tag{116}$$

for the adjoin element $\overline{K} = \bigcup K_i, i = 1, 2, 3, 4.$

Using these postprocessing operators, we can achieve the following global super-convergence for all three dispersive media:

Theorem 3.1. *Assume the partition* T_h *of* Ω *is uniform,* Π_h *and* P_h *are the interpolation on* V_h *and* W_h*, respectively. If* $\mathbf{E} \in C^4(0,T;[H^2(\Omega)]^3)$*,* $\mathbf{H} \in C^4(0,T;[H^2(\Omega)]^3)$*, for the lowest Raviart-Thomas-Nédelec element space, there exists the following super-convergence estimate under the condition that* $\tau \le C_0^* h^2$*:*

$$\max_{1\le n\le N} \|\mathbf{E} - \Pi_{2h}^1 \mathbf{E}_h^n\|_0 \le C(\tau^3 + h^2), \tag{117}$$

$$\max_{1\le n\le N} \|\mathbf{H} - P_{2h}^1 \mathbf{H}_h^n\|_0 \le C(\tau^3 + h^2), \tag{118}$$

in which C *only depends on the exact solution, independent on* τ *and* h*.*

Proof. From (114)-(116), we have

$$\begin{aligned} \|\mathbf{E} - \Pi_{2h}^1 \mathbf{E}_h^n\|_0 &= \|\Pi_{2h}^1(\mathbf{E}_h^n - \Pi_h \mathbf{E}^n) + (\Pi_{2h}^1 \mathbf{E}^n - \mathbf{E}^n)\|_0 \\ &\le C\|\mathbf{E}_h^n - \Pi_h \mathbf{E}^n\|_0 + \|\Pi_{2h}^1 \mathbf{E}^n - \mathbf{E}^n\|_0. \end{aligned} \tag{119}$$

Similarly, we have

$$\begin{aligned} \|\mathbf{H} - P_{2h}^1 \mathbf{H}_h^n\|_0 &= \|P_{2h}^1(\mathbf{H}_h^n - P_h \mathbf{H}^n) + (P_{2h}^1 \mathbf{H}^n - \mathbf{H}^n)\|_0 \\ &\le C\|\mathbf{H}_h^n - P_h \mathbf{H}^n\|_0 + \|P_{2h}^1 \mathbf{H}^n - \mathbf{H}^n\|_0. \end{aligned} \tag{120}$$

From (63) – (68) and Lemma 3.3, we know that the following super-convergence estimate is valid

$$\|g_1^n\|_0,\ \|g_2^n\|_0 \le (\tau^3 + h^2), \tag{121}$$

with C only dependent on $\|\mathbf{E}\|_{C^4(0,T;[H^2(\Omega)]^3)} + \|\mathbf{H}\|_{C^4(0,T;[H^2(\Omega)]^3)}$. This in turn leads to the super-convergent L^2 error estimate for e^n, η^n, in a similar way as (108):

$$\|e^n\|_0^2 + \|\eta^n\|_0^2 \le \widetilde{C_{15}}(\tau^6 + h^{2s}), \tag{122}$$

under the a-priori L^∞ assumption (91). As a result, such an assumption could be similarly recovered as (109):

$$\|e^n\|_{L^\infty} \le \frac{C\|e^n\|_0}{h^{\frac{d}{2}}} \le \frac{\widetilde{C_{15}}(\tau^3 + h^s)}{h^{\frac{d}{2}}} \le C. \tag{123}$$

This finishes the argument for the a-priori bound (91).

Finally, with the help of (114) and (115), we obtain

$$\|\mathbf{E}^n - \Pi_{2h}^1 \mathbf{E}_h^n\|_0 \le Ch^2\|\mathbf{E}^n\|_2,\ \|\mathbf{H}^n - P_{2h}^1 \mathbf{H}_h^n\|_0 \le Ch^2\|\mathbf{H}^n\|_2. \tag{124}$$

The proof of Theorem 3.1 is completed. □

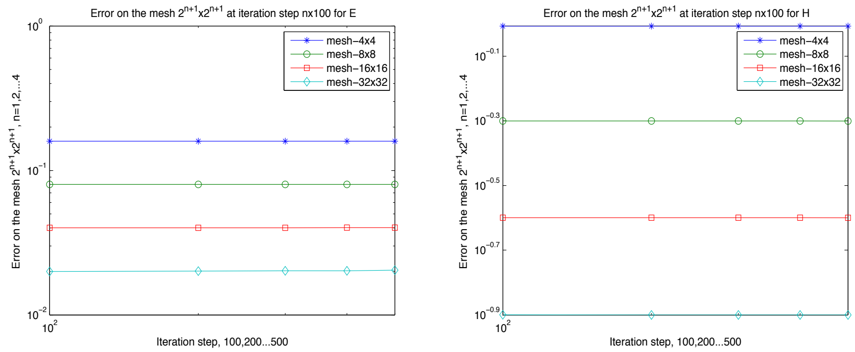

FIGURE 1. Error curve on the mesh $2^{m+1} \times 2^{m+1}$, after $N = 100 : 100 : 500$ time steps.

4. Numerical Results

In this section, we provide some numerical examples in the TE case to confirm our theoretical analysis, with $\mathbf{E} = [E_1, E_2, 0]$ and $\mathbf{H} = [0, 0, H_3]$. For convenience, we still denote $\mathbf{E} = [E_1, E_2]$ and $\mathbf{H} = H_3$. The computations are performed using the Matlab code. The angular frequency is denoted as ω, and the number of time step is given by a sequence: $N = 100 : 100 : 500$. We use the lowest Raviart-Thomas-Nédelec element whose basic functions can be found in the section 3.2 of [17].

In these numerical examples, we observe that, numerical results have shown that, the stability and convergence are well preserved with a more relaxed constraint for the time step, $\tau = O(h)$. The severe time step constraint, $\tau \leq C_0^* h^2$, as appeared in Theorems 2.1, 3.1, is only a theoretical issue.

Define

$$
\begin{aligned}
&errE = \|\mathbf{E}^n - \mathbf{E}_h^n\|_0, \quad errH = \|\mathbf{H}^n - \mathbf{H}_h^n\|_0, \\
&SerrE = \|\mathbf{E}^n - \Pi_{2h}^1 \mathbf{E}_h^n\|_0, \quad SerrH = \|\mathbf{H}^n - \Pi_{2h}^1 \mathbf{H}_h^n\|_0.
\end{aligned}
$$

Example 1: The nonlinear conductivity is fixed as $\sigma(|\mathbf{E}|) = |\mathbf{E}|^2 - |\mathbf{E}|^4$. For $\omega = 1$, the exact solution $(\mathbf{E}, \mathbf{H})$ is formulated as

$$
\begin{aligned}
&\mathbf{E} = [\mathrm{e}^{-t}\cos(\omega\pi x)\sin(\omega\pi y), -\mathrm{e}^{-t}\sin(\omega\pi x)\cos(\omega\pi y)], \\
&\mathbf{H} = -2\omega\pi \mathrm{e}^{-t}\cos(\omega\pi x)\cos(\omega\pi y).
\end{aligned}
$$

The error curves for $\mathbf{E}$ and $\mathbf{H}$ on the mesh $2^{m+1} \times 2^{m+1}$, with $m = 1, 2, 3, 4$, after $N = 100 : 100 : 500$ time steps are provided in Figure 1. The convergence curve is demonstrated in Figure 2 and the numerical solutions are presented in Figure 3.

Example 2: In the case of rectangular mesh, we consider the nonlinear conductivity in the form of $\sigma(|\mathbf{E}|) = |\mathbf{E}|^{1-\alpha}, \alpha = 0.3, 0.5, 0.6, 0.8$, with the exact solution $(\mathbf{E}, \mathbf{H})$ given by

$$
\begin{aligned}
&\mathbf{E} = [(y-1)ye^{-y}\mathrm{e}^{-t}, (x-1)xe^{-x}\mathrm{e}^{-t}], \\
&\mathbf{H} = \mathrm{e}^{-t}(\mathrm{e}^{-x}(-x^2 + 3x - 1) + \mathrm{e}^{-y}(y^2 - 3y + 1)).
\end{aligned}
$$

Figure 4 shows the convergence curve after 100 time steps with $\tau = 10^{-5}$, and $\sigma(|E|) = |E|^{1-\alpha}, \alpha = 0.3, 0.5, 0.6, 0.8$. The numerical solution of $\mathbf{E}$ and $\mathbf{H}$ on the rectangular domain is displayed in Figure 5.

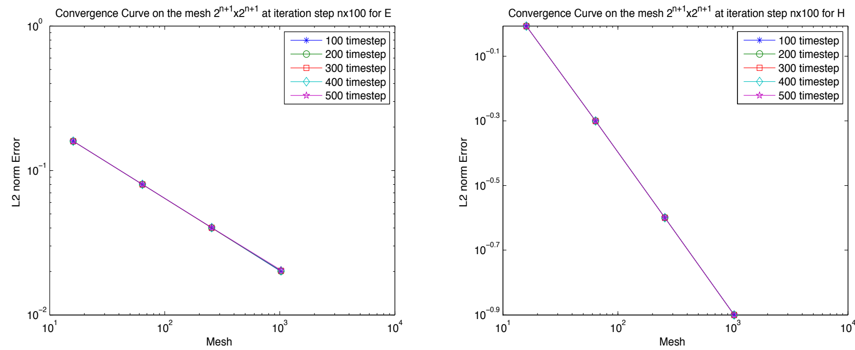

FIGURE 2. Convergence after $N = 100 : 100 : 500$ time steps, with $\tau = 10^{-6}$.

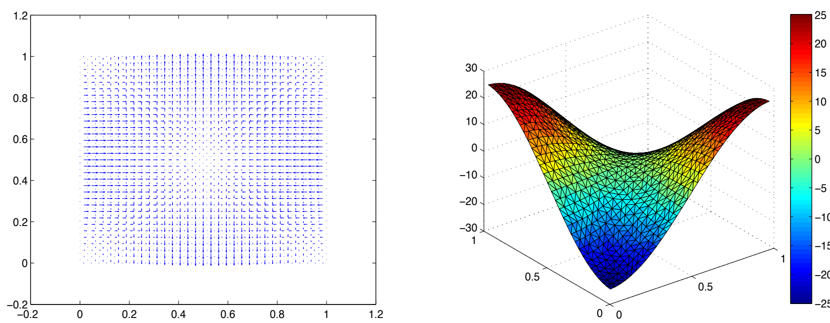

FIGURE 3. Numerical solution for $\mathbf{E}$ and $\mathbf{H}$ with $\sigma(|\mathbf{E}|) = \mathbf{E}^2 - \mathbf{E}^4$.

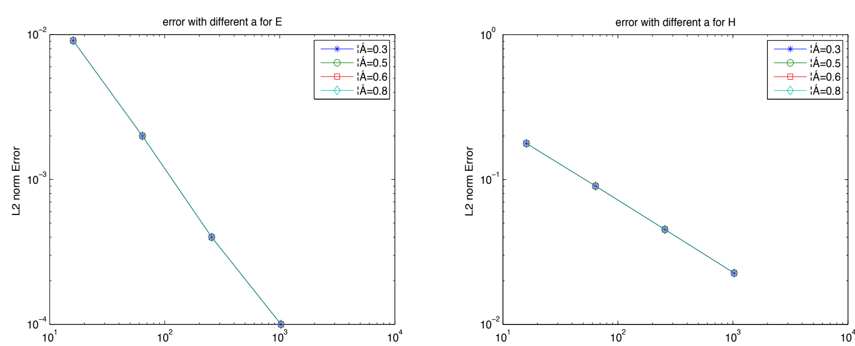

FIGURE 4. Convergence curve after 100 time steps with $\tau = 10^{-5}$, and $\sigma(|E|) = |E|^{1-\alpha}$, $\alpha = 0.3, 0.5, 0.6, 0.8$.

Example 1: In the of an L-shape domain $\Omega = [0,1]^2 \backslash [0.5,1]^2$, we consider the nonlinear conductivity in the form of $\sigma(|\mathbf{E}|) = |\mathbf{E}|^\alpha$, with the initial value

$$\mathbf{E}_0(x, y, 0) = [\sin(2\omega\pi y), \sin(2\omega\pi x)],$$
$$\mathbf{H}_0(x, y, 0) = (-\frac{2\pi\omega}{\mu})(\cos(2\omega\pi x) - \cos(2\omega\pi y)),$$

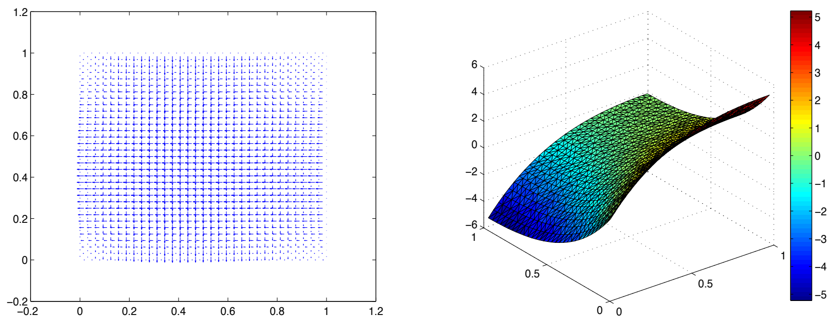

FIGURE 5. Numerical solution for $\mathbf{E}$ and $\mathbf{H}$ with $\sigma(|\mathbf{E}|) = |\mathbf{E}|^{1-\alpha}$,with $\alpha = 0.5$.

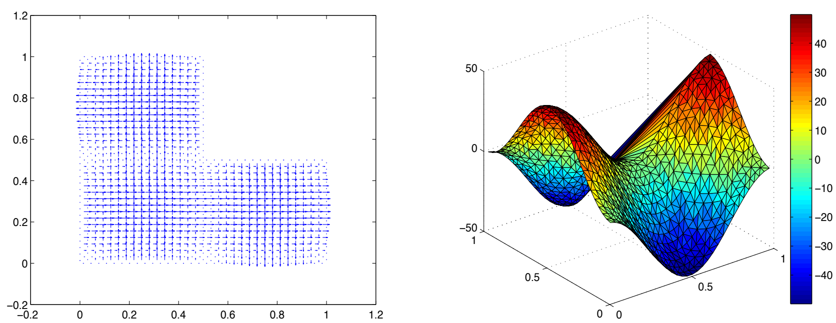

FIGURE 6. Numerical solution of $\mathbf{E}$ and $\mathbf{H}$ on the L-type domain and $\tau = 1e-6$.

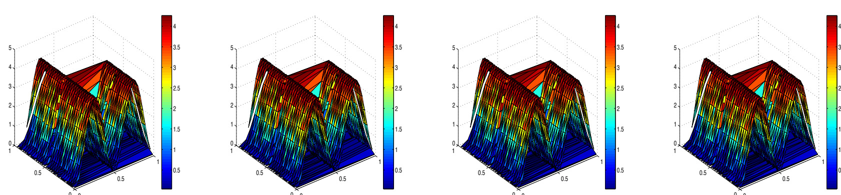

FIGURE 7. The figure of $\sigma(|\mathbf{E}_h^n|) = |\mathbf{E}_h^n|^{\alpha}$, with $\alpha = 0.3, 0.5, 0.6, 0.8$, respectively, at the center of every edge of the element.

and the right-hand-side term

$$
\begin{aligned}
&F(x,y,t) = (f_1, f_2),\\
&f_1 = -\epsilon \mathrm{e}^{-t}\sin(2\omega\pi y) + ((\mathrm{e}^{-t}\sin(2\omega\pi y))^2 + (\mathrm{e}^{-t}\sin(2\omega\pi x))^2)^{\frac{\alpha}{2}}\mathrm{e}^{-t}\sin(2\omega\pi y)\\
&\qquad -\frac{4\pi^2\omega^2}{\mu}\mathrm{e}^{-t}\sin(2\omega\pi y),\\
&f_2 = -\epsilon \mathrm{e}^{-t}\sin(2\omega\pi x) + ((e^{-t}\sin(2\omega\pi y))^2 + (\mathrm{e}^{-t}\sin(2\omega\pi x))^2)^{\frac{\alpha}{2}}\mathrm{e}^{-t}\sin(2\omega\pi x)\\
&\qquad +\frac{4\pi^2\omega^2}{\mu}\mathrm{e}^{-t}\sin(2\omega\pi x).
\end{aligned}
$$

Figure 6 presents the numerical solution of $\mathbf{E}_h^n$ and $\mathbf{H}_h^n$ on the L-shape domain. Meanwhile, the nonlinear conductivity functions $\sigma(|\mathbf{E}_h^n|) = |\mathbf{E}_h^n|^\alpha$, with $\alpha = 0.3, 0.5, 0.6, 0.8$, are displayed in Figure 7, at the center of every edge of the element, respectively.

5. Conclusions

In this article, we propose a third order linearized BDF FEM scheme for the nonlinear Maxwell's equations, with a purely explicit extrapolation applied to the nonlinear terms. Such an explicit treatment has greatly improved the numerical efficiency; only one constant-coefficient linear system needs to be solved at each time step. A theoretical analysis for the 3rd order BDF scheme to the Maxwell's equation turns out to be highly challenging, due to the hyperbolic nature of the equation. We make use of a telescope formula for the 3rd order BDF stencil, combined with other related analytic tools, so that a local in time stability could be derived under a condition for the time step as $\tau \le C_0^* h^2$, with C_0^* a fixed constant. In addition, the linearized stability analysis for the numerical error function has to be performed, which in turn yields the full order L^2 error estimate via an L^∞ a-priori assumption at the previous time steps. As a result, an optimal rate L^2 convergence analysis and error estimate becomes available. Numerical experiments are investigated, which confirm the theoretical analysis.

Acknowledgments

C. Yao is supported by NSFC (NO. 11471296, 11571389, 11101384), Y. Lin is supported by Hong Kong Research Council GRF Grants B-Q56D and 8-ZDA2, and C. Wang is supported by NSF DMS-1418689.

References

[1] A. Buffa, M. Costabel and M. Dauge, Algebraic convergence for anisotropic edge elements in polyhedral domains, Numer. Math., 101, 29-65, 2005.

[2] P. Ciarlet and J. Zou, Fully discrete finite element approaches for time-dependent Maxwell's equations, Numer. Math., 82 (2), 193-219, 1999.

[3] T. Chen, T. Kang, G. Lu and L. Wu, A $(T, \psi) - \psi_e$ decoupled scheme for a time-dependent multiply-connected eddy current problem, Math. Meth. Appl. Sci., 37, 343-359, 2014.

[4] S. Durand and M. Slodička, Convergence of the mixed finite element method for Maxwell's equations with nonlinear conductivity, Math. Meth. Appl. Sci.,35, 1489-1504, 2012.

[5] S. Durand and M. Slodička, Fully discrete finite element method for Maxwell's equations with nonlinear conductivity, IMA J. Numer. Anal., 31, 1713-1733, 2011.

[6] M. V. Ferreira and C. Buriol, Orthogonal decomposition and asymptotic behavior for nonlinear Maxwell's equations, J. Math. Anal. Appl., 426, 392-405, 2015.

[7] H. Gao, Unconditional optimal error estimates of BDF-Galerkin FEMs for nonlinear thermistor equations, J. Sci. Comput, 2015.

[8] H. Gao, Optimal Error Analysis of Galerkin FEMs for nonlinear Joule heating equations, J. Sci. Comput., 58, 627-647, 2014.

[9] Y. Q. Huang, J. C. Li, C. Wu, and W. Yang, Superconvergence analysis for linear tetrahedral edge elements, J. Sci. Comput., 62, 122-145, 2015.

[10] Y. Q. Huang, J. C. Li and W. Yang, Solving metamaterial Maxwell's equations via a vector wave integro-differential equation, Comput. Math. Appl., 63, 1597-1606, 2012.

[11] Y. Q. Huang, J. C. Li and Q. Lin, Superconvergence analysis for time-dependent Maxwell's equations in metamaterials, Numer. Methods Partial Diff. Equ., 28, 1794-1816, 2012.

[12] Y. Q. Huang, J. C. Li and C. Wu, Averaging for superconvergence: verification and application of 2D edge elements to Maxwell's equations in metamaterials, Comput. Meth. Appl. Mech. Engrg. 255, 121-132, 2013.

[13] X. Jiang and W.Y. Zheng, An efficient eddy current model for nonlinear Maxwell equation with laminated conductors, SIAM J. Appl. Math. 72, 1021-1040, 2013.

[14] T. Kang, Y. Wang, L. Wu and K. I. Kim, An improved error estimate for Maxwell's equations with a power-law nonlinear conductivity, Appl. Math. Lett., 45, 93-97, 2015.
[15] B. Li, H. Gao and W. Sun, Unconditionally optimal error estimates of a Crank-Nicolson Galerkin method for the nonlinear thermistor equations, SIAM J. Numer. Anal., 52, 933-954, 2014.
[16] B. Li and W. Sun, Unconditional convergence and optimal error estimates of a Galerkin-mixed FEMs for incompressible miscible flow in porous media, SIAM J. Numer. Anal., 51, 1959-1977, 2013.
[17] J. Li, Y. Huang, Time-domain finite element methods for Maxwell's equations in metamaterials, Springer Science and Business Media, 2012.
[18] Q. Lin and J. C. Li, Superconvergence analysis for Maxwell's equations in dispersive media, Math. Comp., 77, 757-771, 2008.
[19] Q. Lin and J.F. Lin, Finite element methods:accuracy and improvement, Science press, 2006.
[20] J. Liu, Simple and efficient ALE methods with provable temporal accuracy up to fifth order for the Stokes equations on time varying domains, SIAM J. Numer. Anal., 51, 743-772, 2013.
[21] P. Monk, Analysis of a finite-element method for Maxwell equations, SIAM J. Numer. Anal., 29, 714-729, 1992.
[22] P. Monk, A finite-element method for approximating the time-harmonic Maxwell equations, Numer. Math., 63, 243-261,1992.
[23] M. Slodička, A time discretization scheme for a non-linear degenerate eddy current model for free magnetic materials, IMA J. Numer. Anal., 26, 173-187, 2006.
[24] M. Slodička and J. Buša Jr., Error estimates for the time discretization for nonlinear Maxwell's equations, J. Comput. Math., 26, 677-688, 2008.
[25] M. Slodička and S. Durand, Fully discrete finite element scheme for Maxwell's equations with non-linear boundary condition, J. Math. Anal. Appl., 375, 230-244, 2011.
[26] M. Slodička and V. Zemanová, Time-discretization scheme for quasi-static Maxwell's equations with a non-linear boundary condition, J. Comput. Appl. Math., 216, 514-522, 2008.
[27] M.M. Vaǐnberg, L. Alexander and D. Louvish, Variational Method and Method of Monotone Operators in the Theory of Nonlinear Equations, New York, John Wiley,1973.
[28] J. L. Wang, Z. Y. Si and W. W. Sun, A new error analysis of characteristics-mixed FEMs for miscible displacement in porous media, SIAM J. Numer. Anal., 52, 3000-3020, 2014.
[29] J. L. Wang, A new error analysis of Crank-Nicolson Galerkin FEMs for a generalized nonlinear Schrödinger equation, J. Sci. Comput., 60, 390-407, 2014.
[30] C. Yao, Y. Lin and C. Wang, A second order numerical scheme for nonlinear Maxwell's equations using conforming finite element, J. Comput. Math., submitted and in review, 2017.
[31] H. M. Yin, On a Singular limit problem for nonlinear Maxwell's equations, J. Diff. Equ. 156, 355-375, 1999.
[32] H. M. Yin, Existence and regularity of a weak solution to Maxwell's equations with a thermal effect, Math. Meth. Appl. Sci., 29, 1199-1213, 2006.
[33] L. Zhong, S. Shu, G. Wittum and J. Xu, Optimal error estimates for Nedelec edge elements for time-harmonic Maxwell's Equations, J. Comput. Math, 27, 563-572, 2009.

School of Mathematics and Statistics, Zhengzhou University, Zhengzhou, 450001, P.R. China
E-mail: chyao@lsec.cc.ac.cn

Department of Applied Mathematics, Hong Kong Polytechnic University, Hong Kong
E-mail: yanping.lin@ployu.edu.hk

Mathematics Department, The University of Massachusetts, North Dartmouth, MA 02747, USA
E-mail: cwang1@umassd.edu

School of Mathematics and Statistics, Zhengzhou University, Zhengzhou, 450001, P.R. China
E-mail: 422897512@qq.com